Refractory, Ceramic, and Composite Materials
Тугоплавкие, керамические и композиционные материалы

UDC 621.318.122
https://doi.org/10.17073/1997-308X-2024-4-35-44

Research article
Научная статья

Phase transformations, microstructure formation, and magnetic properties of a hysteresis alloy based on the Fe–Cr–Co–Mo system doped with Sm, Zr, and Cu

M. A. Beltyukova✉**, A. A. Shatsov**

Perm National Research Polytechnic University Russia
29 Komsomolskiy Prosp., Perm 614990, Russia

✉ marievamar@rambler.ru

Abstract. The development of new hard magnetic materials (HMM) is crucial for meeting the ever-increasing demands of industry. Today, the advancement of energy, electrical engineering, and instrumentation sectors requires manufacturers of HMM products to enhance the energy efficiency and power of devices while reducing their size and weight, which increases scientists' interest in these alloys. Among HMM, magnets derived from rare-earth elements such as Sm and Nd ($Nd_2Fe_{14}B$, $SmCo_5$, Sm_2Co_{17}) possess the highest magnetic energy at smaller sizes and weights. Alloys based on the Fe–Cr–Co system offer the best reliability, strength, corrosion resistance, and manufacturability, making them particularly in demand among HMM. Creating a magnet based on two alloying systems, Sm–Co and Fe–Cr–Co, may yield a material with unique properties that combine the advantages of both systems. This study investigates the powder hysteresis alloy 22Kh15K4MS (22 % Cr–15 % Ni–4 % Mo–Co–Si) doped with the rare-earth magnet KS25DTs in amounts ranging from 1.5 to 9.0 %. The microstructure, transformation kinetics, phase composition, and magnetic properties of the developed alloys were examined. It was found that the magnetic characteristics of the alloys depend on the concentration of the rare-earth magnet additive and the thermal treatment regime. It was demonstrated that the introduction of 3 % KS25DTs achieves the maximum magnetic properties of the alloy: H_c = 55.6 kA/m, B_r = 1.33 Tl, $(BH)_{max}$ = 41 kJ/m^3. The combination of the developed alloy composition and the thermal treatment regime allows for an increase in the rectangularity coefficient of the magnetic hysteresis loop (K_l) – one of the most important characteristics of precision hysteresis electric motors.

Keywords: hard magnetic material (HMM), powder alloy, magnetic properties, rectangularity coefficient of the magnetic hysteresis loop, Fe–Cr–Co–Mo, Sm–Co.

For citation: Beltyukova M.A., Shatsov A.A. Phase transformations, microstructure formation, and magnetic properties of a hysteresis alloy based on the Fe–Cr–Co–Mo system doped with Sm, Zr, and Cu. *Powder Metallurgy and Functional Coatings*. 2024;18(4): 35–44. https://doi.org/10.17073/1997-308X-2024-4-35-44

Особенности фазовых превращений, формирования микроструктуры и магнитных свойств гистерезисного сплава на основе системы Fe–Cr–Co–Mo, легированного Sm, Zr и Cu

М. А. Бельтюкова ✉, А. А. Шацов

Пермский национальный исследовательский политехнический университет
Россия, 614990, г. Пермь, Комсомольский пр-т, 29

✉ marievamar@rambler.ru

Аннотация. Разработка новых магнитотвердых материалов (МТМ) важна для удовлетворения постоянно растущих требований промышленности. Сегодня развитие энергетической, электротехнической и приборостроительной отраслей требует от производителей изделий из МТМ повышения энергоэффективности, мощности приборов при уменьшении их размеров и массы, что увеличивает интерес ученых к этим сплавам. Среди МТМ наибольшей магнитной энергией при меньших размерах и массе обладают магниты, полученные из редкоземельных элементов, таких как Sm и Nd ($Nd_2Fe_{14}B$, $SmCo_5$, Sm_2Co_{17}). Наилучшие характеристики надежности, прочности, коррозионной стойкости и высокую технологичность изготовления имеют сплавы на основе системы Fe–Cr–Co, что также делает их особенно востребованными среди МТМ. Создание магнита, в основе которого лежат две системы легирования Sm–Co и Fe–Cr–Co, может способствовать получению материала с уникальными свойствами, сочетающего в себе достоинства каждой из указанных систем. В работе исследован порошковый гистерезисный сплав 22Х15К4МС, легированный добавкой редкоземельного магнита марки КС25ДЦ в количестве от 1,5 до 9,0 %. Изучены микроструктура, кинетика превращений, фазовый состав и магнитные свойства разработанных сплавов. Установлено, что магнитные характеристики сплавов зависят от концентрации добавки редкоземельного магнита и режима термической обработки. Показано, что введение сплава КС25ДЦ в количестве 3 % позволяет достичь максимальных магнитных свойств легированного материала: H_c = 55,6 кА/м, B_r = 1,33 Тл, $(BH)_{max}$ = 41 кДж/м^3. Сочетание разработанного состава сплава и режима термической обработки позволяет повысить коэффициент прямоугольности петли магнитного гистерезиса ($K_п$) – одной из важнейших характеристик прецизионных гистерезисных электрических двигателей.

Ключевые слова: магнитотвердый материал (МТМ), порошковый сплав, магнитные свойства, коэффициент прямоугольности петли магнитного гистерезиса, Fe–Cr–Co–Mo, Sm–Co

Для цитирования: Бельтюкова М.А., Шацов А.А. Особенности фазовых превращений, формирования микроструктуры и магнитных свойств гистерезисного сплава на основе системы Fe–Cr–Co–Mo, легированного Sm, Zr и Cu. *Известия вузов. Порошковая металлургия и функциональные покрытия*. 2024;18(4):35–44. https://doi.org/10.17073/1997-308X-2024-4-35-44

Introduction

Recently, there has been a global trend towards producing magnetic materials with enhanced consumer qualities at a lower cost. When comparing rare-earth metal (REM) magnets with magnets from the Fe–Cr–Co system, the former appear less attractive due to their high cost, expensive extraction processes, import dependencies, low mechanical strength, and environmental restrictions during production [1–3]. Research on Fe–Cr–Co-based alloys mainly focuses on reducing the content of expensive elements such as Co [4; 5], and the introduction of micro-additives like Si, Mo, Ti, Dy, Nd, Y, and Sm [6–11].

The greatest interest lies in studies where FCC alloys are doped with REM and W [8; 9–11]. In [9], a cast alloy 43Fe–28Cr–23Co–3Mo–2V–1Zr[1] was doped with 0–3 % yttrium. The best magnetic properties were achieved in the alloy with 2 % Y: the maximum magnetic energy $(BH)_{max}$ increased from 51.3 to 61.6 kJ/m^3, residual magnetic induction (B_r) increased from 0.71 to 1.05 T, and coercive force (H_c) increased from 97 to 130 kA/m compared to the original alloy. Further increase in yttrium content to 3 % led to a decrease in magnetic properties due to phase coarsening and structural heterogeneity. In [10], adding up to 2 % samarium during metallurgical production of cast ingots $(BH)_{max}$ increased by 86 %, B_r by 47 %, and H_c by 28.7 %. The authors attributed this growth in magnetic properties to enhanced shape magnetic anisotropy and magnetic field anisotropy due to intermetallic compounds of the rare-earth magnet $SmCo_5$. Additionally, *X*-ray phase analysis revealed that samarium atoms concentrate in the α_1-phase, thereby increasing the lattice parameter of the strongly magnetic Fe–Co phase and its volume fraction.

Alloys $SmCo_5$ and Sm_2Co_{17} were developed in the 1960s–1980s and are still widely used in valve

[1] Here and throughout the text, mass percent (wt. %) is implied unless otherwise specified.

motors of submersible pumps, flaw detector magnets, magnetic lenses, and couplings [13]. According to research, $SmCo_5$ and Sm_2Co_{17} alloys have high values of magnetocrystalline anisotropy (up to $(15\div20)\cdot10^6$ J/m^3) [14], corrosion resistance (0.1 mg/cm^2 in Na_2S and NaCl, 20 mg/cm^2 in HCl) [15], Curie temperature (727 °C for $SmCo_5$ and 920 °C for Sm_2Co_{17}), and exceed Nd–Fe–B magnets in temperature stability [16–17].

Fe–Cr–Co alloys have already found wide application in mechatronic systems, rotors of high-speed and ultra-high-speed electromechanical energy converters, hysteresis motors, and even microwave radiation absorbers [18–20]. Introducing elements with shape anisotropy of ferromagnetic anisotropic particles, high values of crystal anisotropy constant, and saturation magnetization into Fe–Cr–Co alloys can improve the magnetic properties of the alloy: H_c, B_r, $(BH)_{max}$ [21], and K_l – the rectangularity coefficient of the magnetic hysteresis loop, related by the formula

$$K_l = \frac{B_r}{B_{max}},$$

where B_r is the residual magnetic induction, and B_{max} is the maximum magnetic induction (GOST 19693-74).

Increasing the residual induction of the magnet will allow achieving greater excitation flux while maintaining the torque value in the electric motor with lower armature current, thus increasing the device's efficiency. Due to the demagnetizing factor, the induction at the operating point is lower than B_r, so ensuring the convexity and rectangularity of the magnetic hysteresis loop is essential [22]. Enhancing the power of Fe–Cr–Co hard magnetic alloys will expand their application areas.

The aim of this study is to determine the possibility of improving the magnetic properties of a powder hysteresis hard magnetic alloy based on the Fe–Cr–Co system by doping it with the KS25DTs alloy.

Materials and methods

The study investigated the powder alloy 22Kh15K4MS, doped with the KS25DTs additive in amounts ranging from 0 to 9 % as a substitute for iron (Table 1). The following metal and alloy powders were used as the initial batch components:

– chromium PKh-1S (TU 14-5-298-99) with an average particle size d = 10 μm and a standard deviation σ = 5 μm;

– cobalt GP-OK (TU 1793-008-92), d = 24 μm, σ = 13 μm;

– carbonyl iron OSCh 6-2 (TU 6-09-05808008-262-92), d = 2 μm, σ = 2 μm;

– ferrosilicon FS50 (GOST 1415-93), d = 8 μm, σ = 4 μm;

– molybdenum MPCh (TU 48-19-69-80), d = 2 μm, σ = 1 μm.

Pure samarium powder has low corrosion resistance and a relatively high sintering temperature, so the KS25DTs alloy powder (GOST 21559-76), containing 24–27 % Sm, 1.5–3.5 % Zr, 13–20 % Fe, 4–6 % Cu, and 57.5–43.5 % Co, obtained by crushing magnet scrap, was used in the experiments. Recycling of the sintered $SmCo_5$ alloys, crushed in a hydrogen environment, allows for the production of magnets with an improved microstructure and enhanced magnetic properties compared to the original magnets [23].

All components of the charge were sieved through a 63 μm mesh and homogenized in a mixer with an offset rotation axis for 8 h. The sample billets were obtained by cold pressing in a metal mold in two stages with an intermediate pre-sintering operation. Pressing was carried out at a pressure of 29.4 MPa, followed by pre-sintering at a temperature of 860 °C and holding for 3 h in a hydrogen environment. The samples were then calibrated at a pressure of 34.3 MPa and finally sintered in a vacuum with a residual pressure of 10^{-2} Pa according to the regime t = 1350 °C, τ = 4 h. The density after all sintering stages was determined hydrostatically using a VLR-200 device (Gosmer, Russia) according to GOST 25281-82.

Quenching of all samples was carried out from a temperature of 1250 °C in a 15 % aqueous NaCl solution. Aging of the billets was performed sequentially in 7 stages with the application of an external magnetic field of 150 kA/m. The processing parameters are specified in Table 2. Phase transitions in the studied samples were examined using differential scanning calorimetry (DSC) during the heating and cooling of samples weighing 3–4 g on an STA 449 F3 Jupiter (Netzsch,

Table 1. **Chemical composition of experimental alloys**

Таблица 1. **Химический состав опытных сплавов**

Composition No.	Content, wt. %					
	Fe	Cr	Co	Mo	Si	KS25DTs (Sm)
1	57.5	22.5	15.0	4.0	1.0	0
2	55.5					1.5 (0.36)
3	54.5					3.0 (0.77)
4	53.0					4.5 (1.15)
5	51.5					6.0 (1.53)
6	48.5					9.0 (2.30)

Germany). The heating rate was 10 °C/min. The main parameters and shape of the magnetic hysteresis loop of the experimental samples were determined after quenching and multistage aging using a Permagraph L hysteresis graph (Magnet Physik, Germany) with PERMA software. Experimental data were processed using Fityk and Proteus Analyses software packages (Marcin Wojdyr, Poland).

X-ray phase analysis of the samples was performed using XRD on a D8 Advance ECO powder diffractometer (Bruker, Germany) under the following conditions: cobalt radiation with a wavelength λ = 1,78897 Å, an accelerating voltage of 35 kV, and an *X*-ray tube current of 25 mA.

Qualitative and semi-quantitative analyses were carried out using the Diffrac.Eva software. The PDF-2 2013 powder diffraction database was used for phase identification.

Hardness was measured using a Rockwell hardness tester (Tochpribor, Russia) according to GOST 9013-59 with a load of 150 kg. The microstructure of the samples was investigated using a GX-51 metallographic microscope (Olympus, Japan) with SIAMS 800 software. For high-resolution structural analysis, VEGA 3 (TESCAN, Czech Republic) and FEI Quanta 650FEG (FEI, USA) electron microscopes were used.

Research results

The magnetic characteristics of the 22Kh15K4MS powder alloy are shown in Fig. 1. The base alloy, processed through stages 1 to 7 (Table 2) with the application of an external magnetic field, exhibits the following maximum properties: H_c = 38.9 kA/m, B_r = 1.16 T, $(BH)_{max}$ = 20 kJ/m^3. These properties increased in samples containing KS25DTs additives (with Sm concentrations ranging from 0.36 to 0.77 %), reaching a maximum with the introduction of 0.77 % Sm: H_c = 55.6 kA/m, B_r = 1.33 T, $(BH)_{max}$ = 41 kJ/m^3. However, the magnetic properties deteriorated with an increase in the Sm content from 1.15 to 2.3 % due to phase coarsening [10] and the segregation of samarium at grain boundaries (see Fig. 2, *c*).

Multistage aging of the alloys with the application of an external magnetic field led to the spinodal decomposition of the α-solid solution into the α_1-phase, enriched with iron and cobalt, and the α_2-phase, enriched with chromium. The alternation of the strongly mag-

***Table 2.* Aging mode**

***Таблица 2.* Режимы старения**

Stage No.	*t*, °C	τ, min
1	670	15
2	640	40
3	600	40
4	575	40
5	555	30
6	535	30
7	525	30

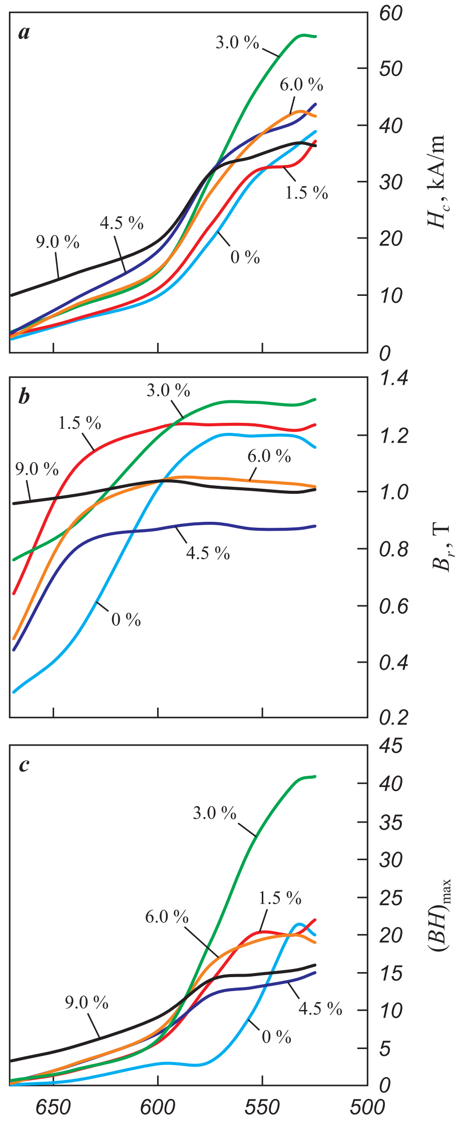

Fig. 1. Dependence of coercive force H_c (***a***), magnetic induction B_r (***b***) and maximum magnetic energy $(BH)_{max}$ (***c***) on the aging temperature of the base alloy 22Kh15K4MS and samples with KS25DTs additive in concentrations ranging from 0 to 9 % (values indicated on the curves)

Рис. 1. Зависимость коэрцитивной силы H_c (***а***), магнитной индукции B_r (***b***) и максимальной магнитной энергии $(BH)_{max}$ (***c***) от температуры старения исходного сплава 22Х15К4МС и образцов с добавкой КС25ДЦ от 0 до 9 % (цифры у кривых)

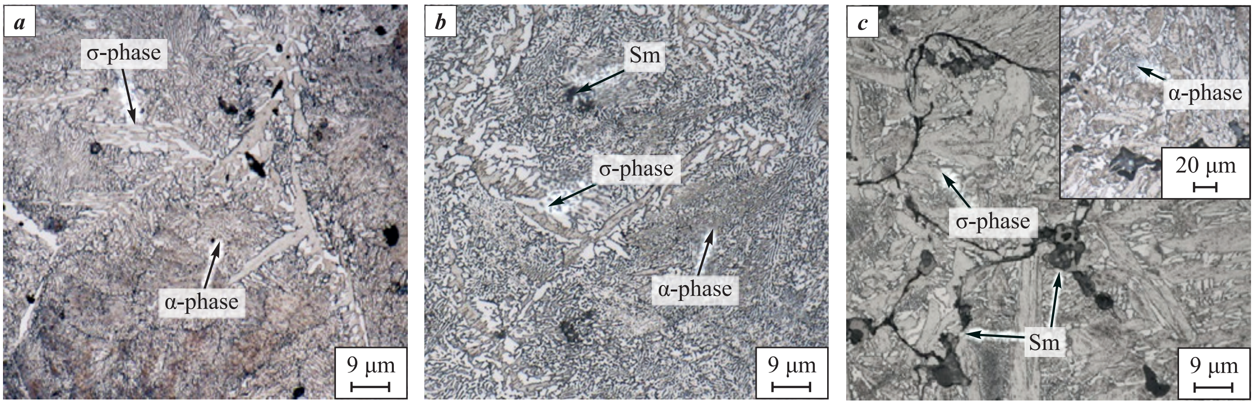

Fig. 2. Microstructure of the alloys after sintering (×1000)
Composition *1* (without additive) (***a***), *3* (***b***) and *6* (***c***) (see Table 1)

Рис. 2. Микроструктура сплавов после спекания (×1000)
Состав *1* (без добавки) (***a***), *3* (***b***) и *6* (***c***) (см. табл. 1)

netic α_1-phase in the weakly magnetic α_2-matrix, along with the presence of samarium-containing phase inclusions that enhance the magnetic anisotropy of the alloy, resulted in increased magnetic properties (H_c, B_r, $(BH)_{max}$) compared to the original sample (see Fig. 1).

The structure of the samples after sintering consists of a lamellar σ-phase, constituting 70–80 vol. %, primarily located at the grain boundaries, with interlayers of the α-phase (Fig. 2). Samarium, appearing as dark areas in the photographs in Fig. 2, *b* and *c*, is also predominantly observed at the grain boundaries.

Due to the presence of the σ-phase, the hardness of the samples after sintering was 35–42 HRC. However, with an increase in the concentration of the KS25DTs additive from 0 to 9 %, the hardness decreased, as did the density (Table 3). The change in porosity exhibited the opposite trend accordingly.

The heating temperature for quenching was selected based on available research results [24] and DSC data. The microstructure of the base alloy after quenching represented an α-solid solution (Fig. 3, *a*). In samples containing the KS25DTs additive, in addition to the α-phase, undissolved Sm inclusions were present (Fig. 3, *b*, *c*).

The hardness of the samples after quenching ranged from 20 to 24 HRC and decreased with an increase in the KS25DTs concentration.

To determine the distribution pattern of the KS25DTs additive in the structure of the 22Kh15K4MS alloy, a sample after quenching was examined using a scanning electron microscope. It was found that the basis of the quenched alloy's structure is an α-solid solution with inclusions containing samarium and zirconium. According to the distribution maps (Fig. 4, *b*), sama-

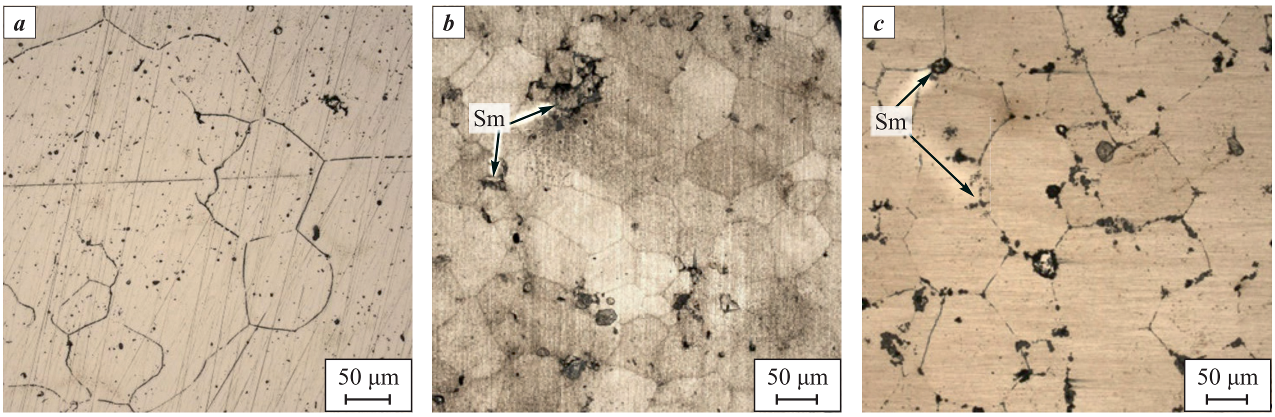

Fig. 3. Microstructure of the alloys after quenching (×1000)
Composition *1* (without additive) (***a***), *3* (***b***) and *6* (***c***) (see Table 1)

Рис. 3. Микроструктура сплавов после закалки (×1000)
Состав *1* (без добавки) (***a***), *3* (***b***) и *6* (***c***) (см. табл. 1)

rium is unevenly distributed within the structure, with areas of accumulation present.

The regions of Sm and Zr distribution overlap when the inclusion size is greater than 1 μm (see Fig. 4, *b*). The authors attribute this to the hindered diffusion processes in the larger initial KS25DTs particles. When the particle size of the additive is below 1 μm, Zr is not detected (Fig. 4, *d*), indicating its uneven distribution in the initial charge material. Regions enriched with Sm are depleted in Co, suggesting partial redistribution of samarium from KS25DTs into the α-solid solution.

The thermal effects during heating of quenched samples, both of the base composition and with the addition of 3 % KS25DTs, exhibited similar kinetics (Fig. 5 *a*, *b*): transformations in both alloys occurred in the temperature range of 500–1100 °C. At 500 °C, spinodal decomposition of the α-phase into strongly magnetic and weakly magnetic phases began, characterized by heat absorption. The addition of 3 % KS25DTs did not significantly affect the position of the first local extremum at around 520 °C. The precipitation of the σ-phase from the solid solution began at 670–680 °C, with the corresponding local extremum recorded at around 700 °C in both samples. The temperature of the third local extremum for the base alloy without the additive was 830 °C, and with the additive, it was 848 °C.

For the alloy with 3 % KS25DTs (Fig. 5, *b*), a curve inflection was observed at 300 °C, which was absent in the base sample. The same peak appeared on the DSC curve of the KS25DTs alloy (Fig. 5, *d*) at 275 °C. According to the study [25], the eutectoid decomposition of $SmCo_5$ into Sm_2Co_7 and Sm_2Co_{17} phases occurs at temperatures below 750 °C, as confirmed by the DSC curve of the KS25DTs alloy (Fig. 5, *d*). When the concentration of the additive in the 22Kh15K4MS alloy was increased to 9 %, an unusual peak at 800 °C was observed on the DSC curve (Fig. 5, *c*).

Thus, the addition of 3 % samarium does not significantly affect the decomposition temperatures of the α-solid solution based on Fe–Cr–Co; however, increasing its concentration to 9 % leads to the appearance of atypical phase transitions in the 22Kh15K4MS alloy.

Table 3. **Density, porosity and hardness of sample blanks after sintering**

Таблица 3. **Плотность, пористость и твердость заготовок образцов после спекания**

Concentration of the KS25DTs, %	Density, g/cm^3	Porosity, %	Hardness, HRC
0	7.9	0.3	42
1.5	7.9	0.5	41
3.0	7.8	1.4	38
4.5	7.7	2.7	39
6.0	7.7	2.7	38
9.0	7.6	4.2	35

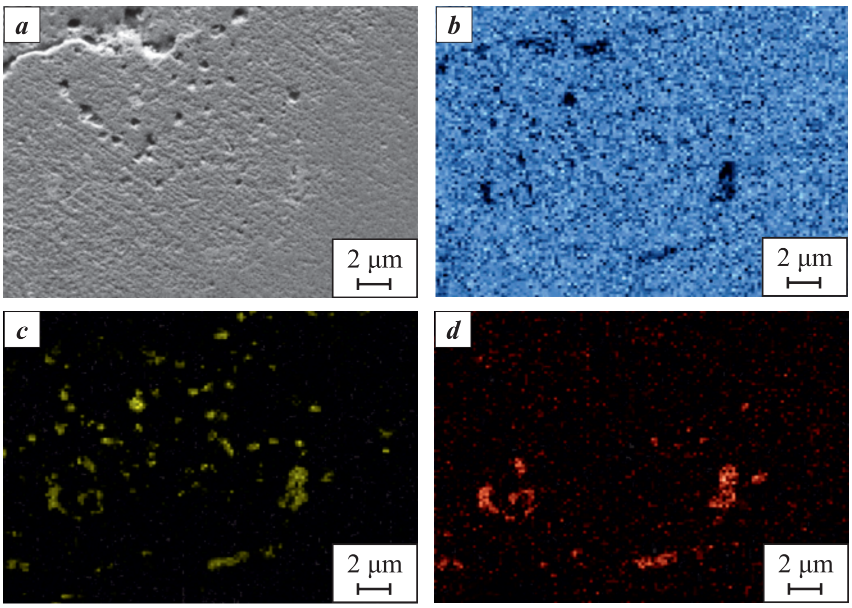

Fig. 4. Microstructure of alloy composition *3* (see Table 1) after quenching (***a***) and distribution maps of Sm (***b***), Co (***c***) and Zr (***d***) in the structure

Рис. 4. Микроструктура сплава состава *3* (см. табл. 1) после закалки (***a***) и карты распределения Sm (***b***), Co (***c***) и Zr (***d***) в структуре

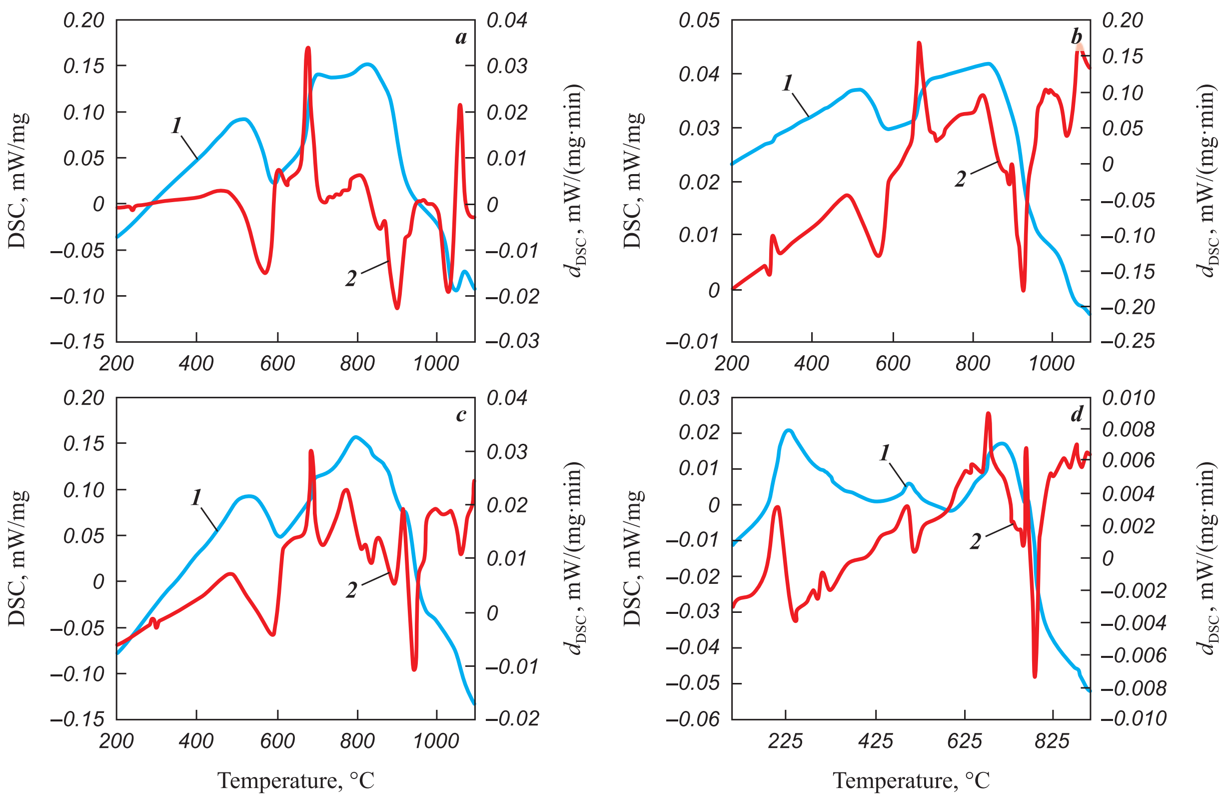

Fig. 5. DSC (*1*) and d_{DSC} (*2*) curves of alloys 22Kh15K4MS (***a***), 22Kh15K4MS + 3 % KS25DTs (***b***), 22Kh15K4MS + 9 % KS25DTs (***c***) and KS25DTs (***d***) when heated at a rate of 10 °C/min

Рис. 5. Кривые ДСК (*1*) и $d_{ДСК}$ (*2*) сплавов 22Х15К4МС (***a***), 22Х15К4МС + 3 % КС25ДЦ (***b***), 22Х15К4МС + 9 % КС25ДЦ (***c***) и КС25ДЦ (***d***) при нагреве со скоростью 10 °С/мин

To evaluate the changes in the phase composition of the 22Kh15K4MS alloy when doped with 3 % KS25DTs, an *X*-ray phase analysis was conducted on the samples after quenching and aging. The results are shown in Fig. 6. The *X*-ray diffraction pattern of the initial sample after quenching shows the presence of the α-phase (2θ = 52.2°). Multistage aging led to a significant increase in magnetic properties. The phase composition after 7 stages of aging underwent the following changes.

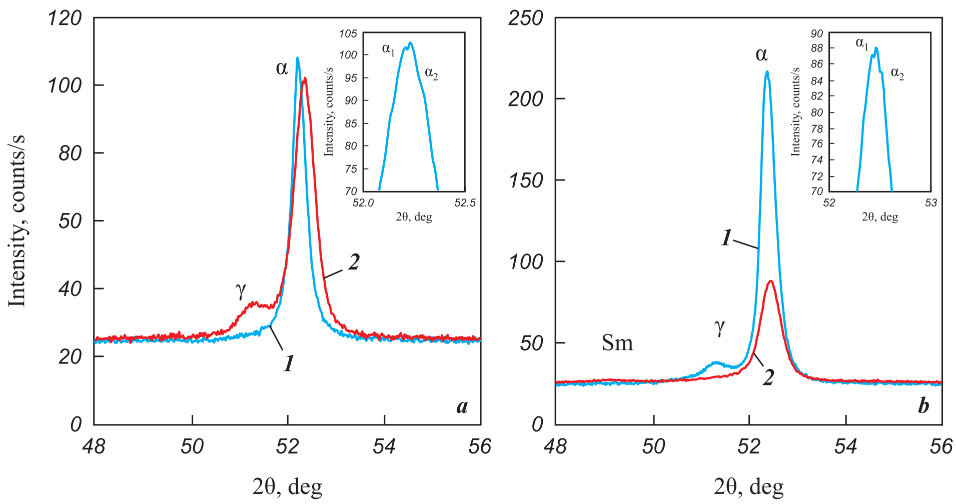

Fig. 6. *X*-ray diffraction patterns of the base 22Kh15K4MS sample (***a***) and with the addition of 3 % KS25DTs (***b***) after quenching (*1*) and thermomagnetic treatment (*2*)

Рис. 6. Рентгенограммы исходного образца 22Х15К4МС (***a***) и с добавкой 3 % КС25ДЦ (***b***) после закалки (*1*) и термомагнитной обработки (*2*)

During aging, the α-phase peak split into two isomorphic phases: α_1, enriched with FeCo, and α_2, based on FeCr. This is noticeable in the 22Kh15K4MS alloy (Fig. 6, *a*) by the increased half-width of the α-phase intensity peaks in the region of 2θ = 52.24°, which is not observed in samples with the KS25DTs additive (Fig. 6, *b*). In the *X*-ray diffraction pattern of the alloy containing the KS25DTs additive, a γ-phase peak (2θ = 51.36°) was detected after quenching, which was absent in the undoped sample (see Fig. 6, *a*). This may indicate a narrowing of the α-solid solution region and a decrease in its stability due to the introduction of alloying additives. A weak peak of the samarium phase with a hexagonal crystal lattice was found at 2θ = 49.2°, which can be explained by its low concentration (23–25 %) in the KS25DTs alloy. This, along with the high values of the crystal anisotropy constant and the saturation magnetization of samarium, led to an increase in the magnetic anisotropy of the doped alloy, contributing to the enhancement of its magnetic properties [10; 21].

Based on *X*-ray phase analysis data, the lattice parameters of the α-phase of the base alloy and the alloy with a 3 % KS25DTs additive are equal and amount to *a* = 2.87 Å. The interplanar distance decreased when doping the 22Kh15K4MS alloy: after quenching, it was 2.032 Å, and in the alloy with a 3 % KS25DTs additive – 2.027 Å. The invariance of the lattice parameter and the decrease in the interplanar distance indicate the absence of Sm dissolution in the α-phase of Fe–Cr–Co system alloys.

To determine the rectangularity coefficient of the magnetic hysteresis loop in the 22Kh15K4MS + 3 % KS25DTs alloy, a sample with a coercive force of 10 kA/m was tested under a remagnetizing field intensity of 100 A/cm (10 kA/m), corresponding to the field intensity of the stator of the hysteresis experimental motor (Fig. 7). The alloy with a 3 % KS25DTs additive was aged according to the first 3 stages of the regime presented in Table 2, with the application of an external magnetic field. The holding time at each stage ranged from 5 to 40 min. The combination of the alloy composition and the thermomagnetic treatment regime ensured high K_l values – up to 0.87.

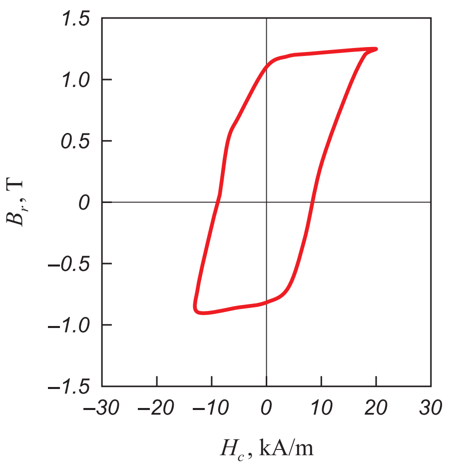

Fig. 7. Magnetic hysteresis loop of the 22Kh15K4MS alloy with 3 % KS25DTs at a magnetizing field intensity H_m = 100 A/cm after aging

Рис. 7. Петля магнитного гистерезиса сплава 22Х15К4МС с 3 % КС25ДЦ при намагниченности магнитного поля H_m = 100 А/см после старения

Thus, increasing the content of the KS25DTs additive from 1.5 to 3 % contributes to changes in the magnetic properties of the 22Kh15K4MS alloy.

Conclusions

The best combination of magnetic hysteresis loop parameters was achieved with a 3 % KS25DTs content in conjunction with thermomagnetic treatment: H_c = 55.6 кА/m, B_r = 1.33 T, and $(BH)_{max}$ = 41 kJ/m^3. However, increasing the KS25DTs additive content from 4.5 % to 9 % results in a decrease in the alloy's magnetic characteristics due to phase coarsening, increased porosity, and the segregation of samarium at the grain boundaries.

Adding up to 3 % KS25DTs does not significantly affect the transformation kinetics of the 22Kh15K4MS alloy. In contrast, increasing the additive concentration from 4.5 % to 9 % leads to the emergence of transformations not typical for this alloy. The presence of Sm phases with high crystal anisotropy constants and saturation magnetization enhances the magnetic characteristics of the doped 22Kh15K4MS alloy.

The combination of the alloy composition with 3 % KS25DTs and the thermomagnetic treatment regime allows for an increased K_l value of 0.87, which may positively influence the dynamic characteristics of precision hysteresis motors in the future.

References / Список литературы

1. Nakamura E., Sato K. Managing the scarcity of chemical elements. *Nature materials*. 2011;10(3):158–161. https://doi.org/10.1038/nmat2969
2. Garganeev A.G., Padalko D.A. Application of Fe–Cr–Co hard magnetic materials as the alternative to Sm–Co and Nd–Fe–B. In: *Proceedings of the 15th International Conference of Young Specialists in the Field of Micro/Nanotechnologies and Electronic Devices* (Novosibirsk, 30 June – 4 July 2014). IEEE. 2014. P. 392–394. https://doi.org/10.1109/EDM.2014.6882555
3. Zhou X., Huang A., Cui B., Sutherland J.W. Techno-economic assessment of a novel SmCo permanent magnet manufacturing method. In: *Proceedings of the 28th CIRP*

Conference on Life Cycle Engineering (India, Jaipur, 10–12 March 2021). 2021. Vol. 98(2). P. 127–132. https://doi.org/10.1016/j.procir.2021.01.017

4. Belozerov E.V., Mushnikov N.V., Ivanova G.V., Shchegoleva N.N., Serikov V.V., Klejnerman N.M., Vershinin A.V., Ujmin M.A. High-strength magnetic hard alloys based on Fe–Cr–Co with a reduced content of chromium and cobalt. *Fizika metallov i metallovedenie*. 2012;113(4): 339–346. (In Russ.).

   Белозеров Е.В., Мушников Н.В., Иванова Г.В., Щеголева Н.Н., Сериков В.В., Клейнерман Н.М., Вершинин А.В., Уймин М.А. Высокопрочные магнитотвердые сплавы на основе Fe–Cr–Co с пониженным содержанием хрома и кобальта. *Физика металлов и металловедение*. 2012;113(4):339–346.

5. Gao Q. Gong M., Wang Y., Qu F., Huang J. Phase transformation and properties of Fe–Cr–Co alloys with low cobalt content. *Materials Transactions*. 2015;56(9):1491–1495. https://doi.org/10.2320/matertrans.M2015077

6. Alymov M. I., Ankudinov A.B., Zelenskii V.A., Milyaev I.M., Yusupov V.S., Ustyuhin A.S.. Influence of alloying and sintering mode on magnetic hysteresis properties of Fe–Cr–Co powder alloy. *Fizika i khimiya obrabotki materialov*. 2011;3:34–37. (In Russ.).

   Алымов М. И., Анкудинов А.Б., Зеленский В.А., Миляев И.М., Юсупов В.С., Устюхин А.С. Влияние легирования и режима спекания на магнитные гистерезисные свойства Fe–Cr–Co порошкового сплава. *Физика и химия обработки материалов*. 2011;3:34–37.

7. Milyaev I.M., Alymov M.I., Yusupov V.S., Ankudinov A.B., Zelenskii V.A., Milyaev A.I. The influence of silicon and molybdenum on the magnetic hysteresis properties of the magnetic hard powder alloy 22X15KA. *Powder Metallurgy and Functional Coatings*. 2011;(4):54–57. (In Russ.). https://powder.misis.ru/jour/issue/view/34

   Миляев И.М., Алымов М.И., Юсупов В.С., Анкудинов А.Б., Зеленский В.А., Миляев А.И. Влияние кремния и молибдена на магнитные гистерезисные свойства магнитотвердого порошкового сплава 22Х15КА. *Известия вузов. Порошковая металлургия и функциональные покрытия*. 2011;(4):54–57. https://powder.misis.ru/jour/issue/view/34

8. Ustyukhin A.S., Zelenskii V.A., Milyaev I.M., Alymov M.I., Kovalev D.Y., Shustov V.S. Magnetic hysteresis properties of isotropic hard magnetic Fe–Cr–Co compositions alloyed with tungsten. *Russian Metallurgy (Metally)*. 2023;7: 933–939. https://doi.org/10.1134/S003602952307011X

9. Tao S., Ahmad Z., Zhang P., Zheng X., Wang F., Xu X. Enhancement of magnetic and microstructural properties in Fe–Cr–Co–Mo–V–Zr–Y permanent magnetic alloy. *Journal of Magnetism and Magnetic Materials*. 2019;484: 88–94. https://doi.org/10.1016/j.jmmm.2019.04.004

10. Tao S., Ahmad Z., Zhang P., Zheng X., Zhang S. Effects of Sm on structural, textural and magnetic properties of Fe–28Cr–20Co–3Mo–V–2Ti hard magnetic alloy. *Journal of Alloys and Compounds*. 2020;816:152619. https://doi.org/10.1016/j.jallcom.2019.152619

11. Ustyukhin A.S., Zelenskii V.A., Milyaev I.M., Yusupov B.S., Alymov M.I., Kovalev D.Y. The Influence of molybdenum and titanium on magnetic and mechanical properties of Fe–30Cr–16Co (Kh30K16) powder hard magnetic alloy. *Steel in Translation*. 2021;51(12):939–944. https://doi.org/10.3103/S0967091221120135

12. Han X.H., Sun J.B., Yu X., Wang S., Chen S.Y., Zhang Y., Cui C.X. Effects of annealing and magnetic field on the structure and magnetic properties of Fe–Cr–Co alloy-doped Sm $(Co_{0.9}Cu_{0.1})_5$ ribbons. *Journal of Magnetism and Magnetic Materials*. 2020;515:167308. https://doi.org/10.1016/j.jmmm.2020.167308

13. Korol' V. I., Lankin I. M., Lankin M. V. Application of permanent magnets in various industries. *Vestnik molodyozhnoy nauki Rossii*. 2020;5:3–13. (In Russ.).

    Король В.И., Ланкин И.М., Ланкин М.В. Применение постоянных магнитов в разных отраслях. *Вестник молодежной науки России*. 2020;5:3–13.

14. Larson P., Mazin I. I. Magnetic properties of $SmCo_5$ and YCo_5. *Journal of Applied Physics*. 2003;93(10): 6888–6890. https://doi.org/10.1063/1.1556154

15. Tsutsui H., Kinouchi Y., Sasaki H., Shiota M., Ushita T. Studies on the Sm–Co magnet as a dental material. *Journal of Dental Research*. 1979;58(6):1597–1606. https://doi.org/10.1177/00220345790580060901

16. Liu J. F., Walmer M. H. Thermal stability and performance data for SmCo 2:17 high-temperature magnets on PPM focusing structures. *IEEE Transactions on Electron Devices*. 2005;52(5):899–902. https://doi.org/10.1109/TED.2005.845868

17. Haavisto M., Paju M. Temperature stability and flux losses over time in sintered Nd–Fe–B permanent magnets. *IEEE Transactions on Magnetics*. 2009;45(12):5277–5280. https://doi.org/10.1109/TMAG.2009.2023907

18. Delektorskii B.A., Tarasov V.N. Controlled hysteresis electric drive. Moscow: Energoatomizdat, 1983. 128 p. (In Russ.).

    Делекторский Б.А., Тарасов В.Н. Управляемый гистерезисный привод. М.: Энергоатомиздат, 1983. 128 с.

19. Nikanorov V.B., Ostanin S.Yu., Shmeleva G.A. Modeling of magnetization reversal processes of unstabilized magnetically hard materials *Elektrichestvo*. 2002;11:28–36. (In Russ.).

    Никаноров В.Б., Останин С.Ю. Шмелева Г.А. Моделирование процессов перемагничивания нестабилизированных магнитно-твердых материалов. *Электричество*. 2002;11:28–36.

20. Ajia S., Asa H., Toyoda Y., Sato M., Matsuura M., Tezuka N., Sugimoto S. Development of an alternative approach for electromagnetic wave absorbers using Fe–Cr–Co alloy powders. *Journal of Alloys and Compounds*. 2022;903:163920. https://doi.org/10.1016/j.jallcom.2022.163920

21. Burhanov G.S., Milyaev I.M., Yusupov V.S. Current state and development trends of magnetic hard materials. *Perspektivnye materialy*. 2011;11:208–215. (In Russ.). https://www.elibrary.ru/item.asp?id=17561313

    Бурханов Г.С., Миляев И.М., Юсупов В.С. Современное состояние и тенденции развития магнитотвёрдых материалов. *Перспективные материалы*. 2011;11: 208–215. https://www.elibrary.ru/item.asp?id=17561313

22. Nagajcev V.I., Sergeev S.V., Sizyakin A.V. Evolution of requirements to the material properties of permanent magnets for electrical machines. *Vestnik Yuzhno-Ural'skogo*

gosudarstvennogo universiteta. Seriya: Energetika. 2021; 21(1):99–108. https://doi.org/10.14529/power210111

Нагайцев В.И., Сергеев С.В., Сизякин А.В. Эволюция требований к свойствам материалов постоянных магнитов для электрических машин. *Вестник Южно-Уральского государственного университета. Серия: Энергетика*. 2021;21(1):99–108. https://doi.org/10.14529/power210111

23. Eldosouky A., Škulj I. Recycling of $SmCo_5$ magnets by HD process. *Journal of Magnetism and Magnetic Materials*. 2018;454:249–253. https://doi.org/10.1016/j.jmmm.2018.01.064

24. Korznikov A.V., Korznikova G.F., Gladkovskij S.V., Potekaev A.I., Dmitriev S.V. The effect of the heat treatment regime on the structure and physical and mechanical properties of the magnetohard alloy 23X15KT. *Izvestija vysshikh uchebnykh zavedeniy. Fizika*. 2014;57(10):10–14. (In Russ.). https://www.elibrary.ru/item.asp?id=22754364

Корзников А.В., Корзникова Г.Ф., Гладковский С.В., Потекаев А.И., Дмитриев С.В. Влияние режима термообработки на структуру и физико-механические свойства магнитотвердого сплава 23Х15КТ. *Известия высших учебных заведений. Физика*. 2014;57(10):10–14. https://www.elibrary.ru/item.asp?id=22754364

25. Menushenkov V.P. Structural transformations and coercive force in permanent magnet alloys. Part 2. Sintered alloys based on Sm–Co and Nd–Fe–B. *Gornyy informatsionno-analiticheskiy byulleten' (nauchno-tekhnicheskii zhurnal)*. 2007; (S1):163–178. (In Russ.). https://www.elibrary.ru/item.asp?id=15196761

Менушенков В.П. Структурные превращения и коэрцитивная сила в сплавах для постоянных магнитов. Часть 2. Спеченные сплавы на основе Sm–Co и Nd–Fe–B. *Горный информационно-аналитический бюллетень (научно-технический журнал)*. 2007;(S1):163–178. https://www.elibrary.ru/item.asp?id=15196761

Information about the Authors

Maria A. Beltyukova – Postgraduate Student of the Department of Metal Science, Thermal and Laser Processing of Metals, Perm National Research Polytechnic University
ORCID: 0000-0002-6599-5091
E-mail: marievamar@rambler.ru

Alexander A. Shatsov – Dr. Sci. (Eng.), Professor of the Department "Metal science, heat and laser treatment of metals", Perm National Research Polytechnic University
ORCID: 0000-0002-2723-964X
E-mail: shatsov@pstu.ru

Сведения об авторах

Мария Александровна Бельтюкова – аспирант кафедры «Металловедение, термическая и лазерная обработка металлов», Пермский национальный исследовательский политехнический университет (ПНИПУ)
ORCID: 0000-0002-6599-5091
E-mail: marievamar@rambler.ru

Александр Аронович Шацов – д.т.н., профессор кафедры «Металловедение, термическая и лазерная обработка металлов», ПНИПУ
ORCID: 0000-0002-2723-964X
E-mail: shatsov@pstu.ru

Contribution of the Authors

M. A. Beltyukova – preparation of the mixture and initial samples, conducting experiments, writing the manuscript.
A. A. Shatsov – defining the study's objective, participating in the discussion of results, editing the manuscript.

Вклад авторов

М. А. Бельтюкова – подготовка смеси и исходных образцов, проведение экспериментов, написание текста статьи.
А. А Шацов – определение цели работы, участие в обсуждении результатов, корректировка текста статьи.

Received 27.07.2023
Revised 12.03.2024
Accepted 15.03.2024

Статья поступила 27.07.2023 г.
Доработана 12.03.2024 г.
Принята к публикации 15.03.2024 г.